TECHNICAL MEMORANDUM

X-521

DECLASSIFIED- AUTHORITY
US: 663 DROBKA TO LEBOW
MEMO DATED 2/1/66
1/10/66

STATIC LONGITUDINAL AND LATERAL

AERODYNAMIC CHARACTERISTICS AT A MACH NUMBER OF 2.20 OF A

V/STOL AIRPLANE CONFIGURATION WITH A VARIABLE-SWEEP WING

AND WITH A SKEWED WING DESIGN

By Odell A. Morris and Gerald V. Foster

Langley Research Center
Langley Field, Va.

GPO PRICE $ _____

CFSTI PRICE(S) $ _____

Hard copy (HC) _____

Microfiche (MF) _____

653 July 65

NATIONAL AERONAUTICS AND SPACE ADMINISTRATION

WASHINGTON   April 1961

NATIONAL AERONAUTICS AND SPACE ADMINISTRATION

TECHNICAL MEMORANDUM X-521

STATIC LONGITUDINAL AND LATERAL

AERODYNAMIC CHARACTERISTICS AT A MACH NUMBER OF 2.20 OF A

V/STOL AIRPLANE CONFIGURATION WITH A VARIABLE-SWEEP WING

AND WITH A SKEWED WING DESIGN[*]

By Odell A. Morris and Gerald V. Foster

SUMMARY

2375

An investigation has been conducted in the Langley 4- by 4-foot
supersonic pressure tunnel at a Mach number of 2.20 to determine the
static longitudinal and lateral aerodynamic characteristics of a
V/STOL airplane configuration with a variable-sweep wing having out-
board panels swept back 75° and with a skewed wing having wing skew
angles of 0°, 30°, 60°, and 90°.

The results show a linear variation of the pitching-moment coeffi-
cient with lift coefficient for both the configuration with a 75° swept
wing and the skewed-wing configuration for wing skew angles up to 30°.
Increasing the wing skew angle from 30° to 90° produced nonlinear
pitching-moment curves with a sizable positive trim change. Both model
configurations had unstable directional characteristics above angles of
attack of approximately 2°.

INTRODUCTION

The National Aeronautics and Space Administration is currently con-
ducting configuration studies directed toward the development of an effi-
cient multimission V/STOL airplane capable of operation at both subsonic
and supersonic speeds. Results of recent studies indicate that configu-
rations incorporating variable wing sweep designs provide one type of
aircraft capable of efficient operation at subsonic and supersonic
speeds. (See refs. 1 to 5.) As pointed out in reference 5 the added

---

[*]Title, Unclassified.
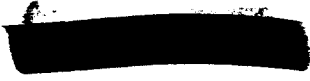
requirement of low-level supersonic dash ability has indicated the desirability of sweeping the wing to such an extent that a large portion of the wing is confined within or on top of the fuselage. Such an arrangement would allow a considerable reduction in the drag and gust accelerations associated with flight at high dynamic pressures. In order to fulfill this design feature a skewed wing arrangement has been suggested as an alternate to the fully sweptback wing arrangement.

Accordingly, an investigation has been conducted in the Langley 4- by 4-foot supersonic pressure tunnel at a Mach number of 2.20 of two V/STOL airplane configurations designed about a proposed vectored lift-thrust engine. These configurations differed only in wing design - one having a variable-sweep wing with the outboard panels fixed at 75° and the other having a skewed wing arrangement with provisions for skew angles of 0°, 30°, 60°, and 90°. The results of the investigation, together with a limited analysis, are presented herein.

SYMBOLS

All force and moment coefficients are referred to the body-axis system except the lift and drag coefficients which are referred to the wind-axis system. Data for the variable-sweep wing are based on the wing geometry with the outboard panels swept back 75°. Data for the skewed wing are based on the wing geometry when the wing skew angle is 0°. The moment reference point is located 0.7 inch above the fuselage reference line at a station 50.5 percent of the body length.

C_D drag coefficient, $\dfrac{\text{Drag}}{qS}$

C_L lift coefficient, $\dfrac{\text{Lift}}{qS}$

C_m pitching-moment coefficient, $\dfrac{\text{Pitching moment}}{qS\bar{c}}$

C_l rolling-moment coefficient, $\dfrac{\text{Rolling moment}}{qSb}$

C_{l_β} effective dihedral parameter, $\dfrac{\partial C_l}{\partial \beta}$

C_n yawing-moment coefficient, $\dfrac{\text{Yawing moment}}{qSb}$

C_{n_β} directional-stability parameter, $\dfrac{\partial C_n}{\partial \beta}$

C_Y side-force coefficient, $\dfrac{\text{Side force}}{qS}$

C_{Y_β} side-force parameter, $\dfrac{\partial C_Y}{\partial \beta}$

L/D lift-drag ratio, C_L/C_D

S wing area including fuselage intercept

b wing span

$\bar{c}$ wing mean geometric chord

q free-stream dynamic pressure

α angle of attack, deg

β angle of sideslip, deg

δ_h horizontal-tail deflection, deg

MODEL AND APPARATUS

Details of the model configurations are shown by drawings and photographs presented in figures 1 and 2, respectively. The model had a large single scoop-type inlet below the nose of the fuselage which had a total capture area of 7.15 sq in. Four jet exits (two on each side) were located on the bottom of fuselage approximately below the wing root. Each of the two forward jet exits had an exit area of 1.255 sq in., and each of the two rearward exits had an exit area of 1.90 sq in. The vertical and horizontal tail surfaces were constructed of 1/8-inch-thick flat steel plate with rounded leading edges and beveled trailing edges.

The model was tested with two different wing planforms. One plan-form, which had a variable-sweep design, had a leading-edge sweep angle fixed at 60° on the inboard panels, whereas the sweepback angle of the outboard sections was 75°. With the outboard panels swept back 25°, the airfoil sections (streamwise) of the outboard panel were 6 percent thick with a flat lower surface and an upper surface which conformed
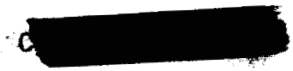
to the upper surface ordinates of the NACA 65_1A012 airfoil section.

The leading edge was rounded with a radius of approximately .64 percent of the wing chord. The skewed wing had a trapezoidal planform with airfoil sections 3 percent thick which had a circular-arc upper surface and a flat lower surface with a small leading-edge radius. The skewed wing was designed so that the wing could be rotated about a point located at 50 percent of the root chord from 0° skew angle (wing tips parallel to body center line) to 90° skew angle (wing tips perpendicular to body center line). The model was mounted on a remotely controlled rotary sting, and force measurements were made through the use of a six-component internal strain-gage balance.

TESTS, CORRECTIONS, AND ACCURACY

The test conditions are as follows:

Mach number 2.20
Stagnation temperature, °F 110
Stagnation pressure, lb/sq ft 1,440
Reynolds number per foot . . . . 2.20 × 10⁶

The stagnation dewpoint was maintained sufficiently low (-25° F or less) to prevent condensation effects in the test section. Tests were made through an angle-of-attack range at $\beta = 0°$, 4.2°, 8.3°, and 12.5°. The angles of attack and sideslip were corrected for deflection of the balance and sting under load. The pressure within the balance enclosure was measured, and the drag force was adjusted to a balance chamber pressure equal to free-stream static pressure. The internal-drag correction applied to the drag results presented herein varied with angle of attack from approximately 0.0110 to 0.0160. Pressure measurements at the nacelle exits showed supersonic exit flow, but for the calculation of the internal-drag correction, sonic flow at the nacelle exit was assumed. Erratic behavior of the drag results presented herein are believed to be the result of flow separation within the duct.

In order to insure a turbulent boundary layer, 1/8-inch-wide strips of No. 80 carborundum grains were attached to the wing and tail surfaces at the 0.10-chord station and at a body station 1 inch rearward of the nose.
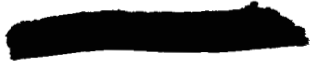
The estimated accuracy of the measured quantities is as follows:

C_L . . . . ±0.0050

C_D . . . . ±0.0020

C_m . . . . ±0.0020

C_l . . . . ±0.0002

C_n . . . . ±0.0012

C_Y . . . . ±0.0053

α, deg . . . . ±0.1

β, deg . . . . ±0.1

δ_h, deg . . . . ±0.1

PRESENTATION OF RESULTS

The results of the investigation and the figures in which they are presented are listed in the following table:

SUMMARY OF RESULTS

The data of figures 3 and 4 show that the pitching-moment curves varied linearly with C_L for the configuration with the 75° swept wing and also for the skewed-wing configuration when the wing skew angle
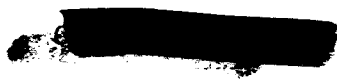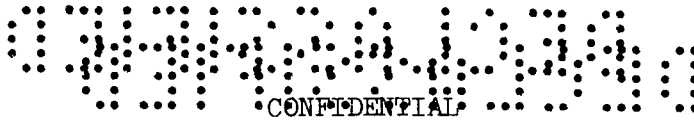
was 0° The pitching-moment results indicate a static margin of 25 percent $\bar{c}$ for the configuration with the 75° swept wing and 30 percent $\bar{c}$ for the skewed-wing configuration with a skew angle of 0°.

Comparison of the drag coefficients for these two configurations (figs. 3 and 4) shows that the configuration with the 75° swept wing had a minimum drag-coefficient value of 0.038, which was less than the minimum drag-coefficient value (0.065, based on skewed-wing area; or 0.044 when based on swept-wing area) for the skewed-wing configuration (0° skew angle). The maximum value of untrimmed lift-drag ratio for the configuration with the 75° swept wing was 4.3 as compared with a value of 3.8 for the skewed-wing configuration.

The data of figure 6 show the effect of wing skew angle on the aerodynamic characteristics in pitch for the skewed-wing configuration. Rotation of the wing skew angle from 0° to 90° resulted in nonlinear pitching-moment curves with sizable positive trim change above a wing skew angle of 30°. The minimum value of drag coefficient was decreased from 0.065 to 0.055 with a corresponding large decrease in the lift-curve slope. The maximum value of untrimmed L/D was also decreased from 3.8 to 3.2 as a result of increased wing skew.

The effects of angle of attack on the sideslip derivatives have been obtained from figures 7 and 8 for both wing configurations and are summarized in figures 9 and 10. The results indicate that the model is directionally unstable above an angle of attack of approximately 2° with either wing configuration and that C_{n_β} continues to decrease rapidly with further increases in angle of attack. The unstable model characteristics were probably caused by inadequate vertical-tail area as a result of the large portion of lateral area forward of the model moment center. The results for the configuration with the 75° swept wing indicate an increase in the positive effective dihedral $\left(-C_{l_\beta}\right)$ whereas the results for the skewed-wing configuration show a general decrease in $-C_{l_\beta}$ with increasing angle of attack.

Variation of the wing skew angle from 0° to 90° for the skewed-wing configuration produced relatively small variations in C_{n_β} and C_{Y_β} with increases in angle of attack; however, the variations in C_{l_β} due to wing rotation were somewhat larger.

Langley Research Center,
      National Aeronautics and Space Administration,
            Langley Field, Va., January 31, 1961.
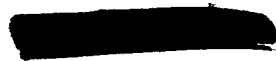
REFERENCES

1. Spencer, Bernard, Jr.: Stability and Control Characteristics at Low Subsonic Speeds of an Airplane Configuration Having Two Types of Variable-Sweep Wings. NASA TM X-303, 1960.

2. Foster, Gerald V., and Morris, Odell A.: Aerodynamic Characteristics in Pitch at a Mach Number of 1.97 of Two Variable-Wing-Sweep V/STOL Configurations With Outboard Wing Panels Swept Back 75°. NASA TM X-322, 1960.

3. Luoma, Arvo A., and Alford, William J., Jr.: Performance, Stability, and Control Characteristics at Transonic Speeds of Three V/STOL Airplane Configurations With Wings of Variable Sweep. NASA TM X-321, 1960.

4. Foster, Gerald V., and Morris, Odell A.: Static Longitudinal and Lateral Aerodynamic Characteristics at a Mach Number of 2.20 of a Variable-Wing-Sweep STOL Configuration. NASA TM X-329, 1960.

5. Bielat, Ralph P., Robins, A. Warner, and Alford, William J., Jr.: The Transonic Aerodynamic Characteristics of Two Variable-Sweep Airplane Configurations Capable of Low-Level Supersonic Attack. NASA TM X-304, 1960.

When outboard wing sweep = 75°
$S = 0.858$ sq ft
$\bar{c} = 0.740$ ft
$b = 1.309$ ft
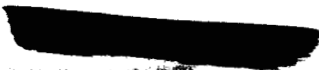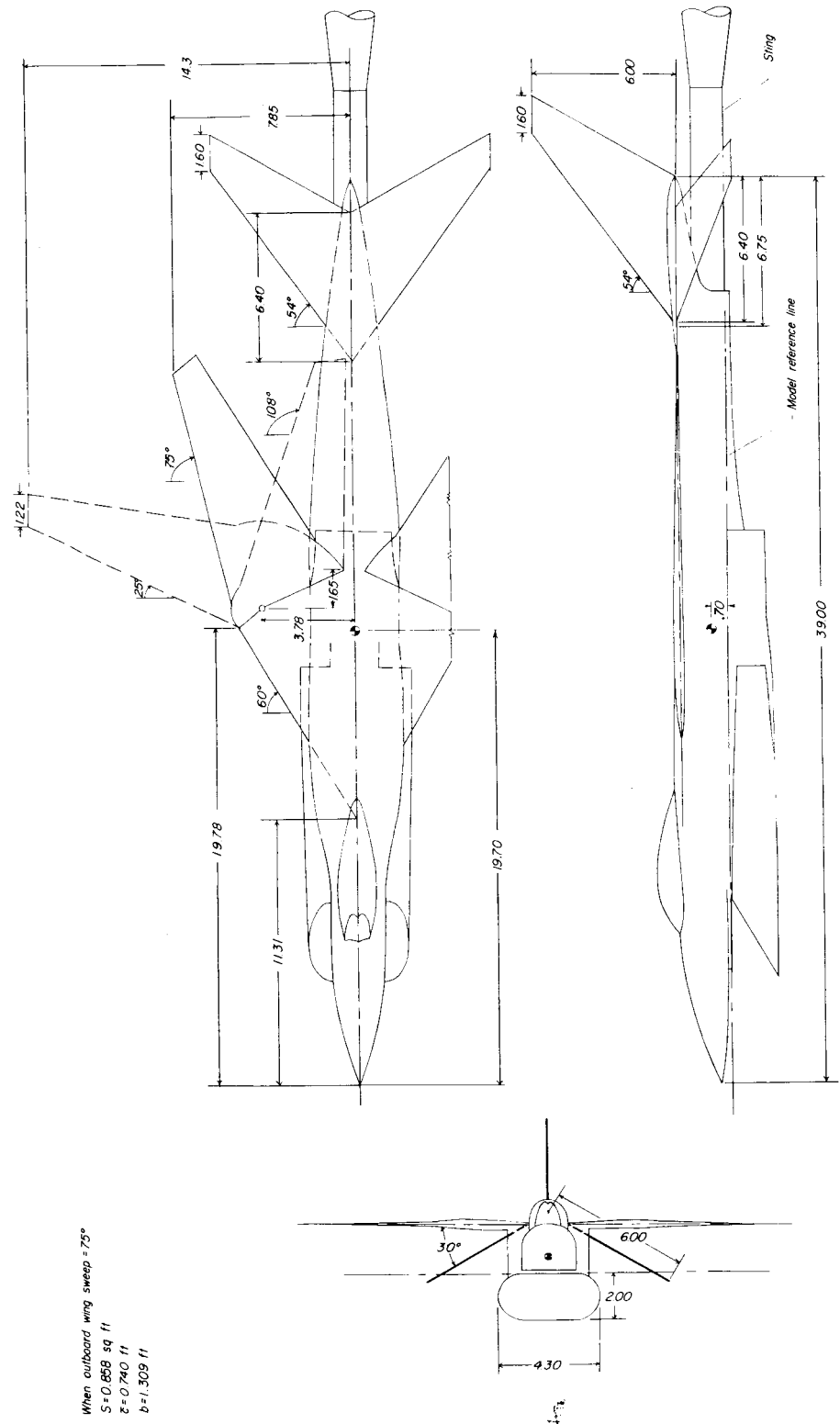
(a) Configuration with 75° swept wing. All dimensions are in inches unless otherwise indicated.

Figure 1.- Details of model configurations.

L-1458

S = 0.586 sq ft
c̄ = 0.431 ft
b = 1.562 ft

21.89

9.38

3.75

17.5°

1.50

.2.19

Skew angle = 90°

Skew angle = 0°
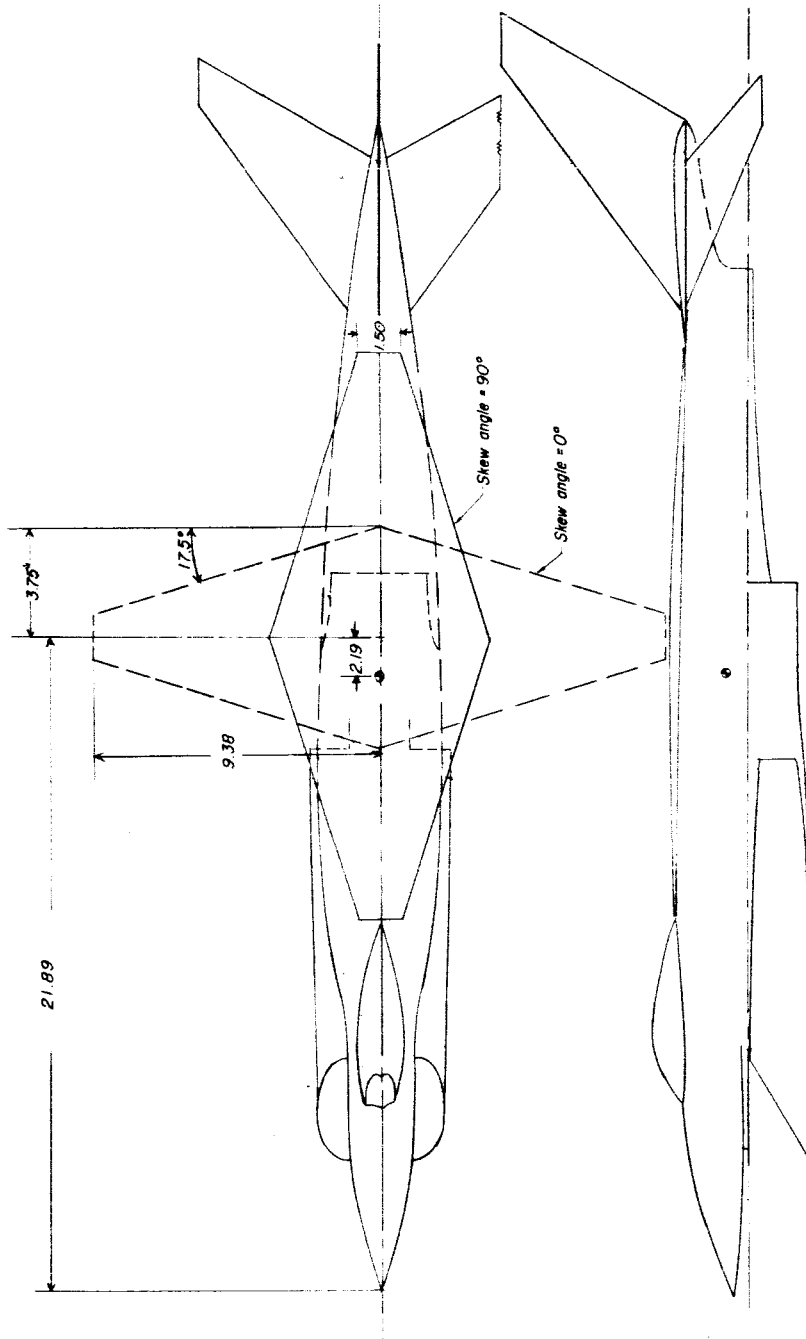
(b) Skewed-wing configuration.

Figure 1.- Concluded.
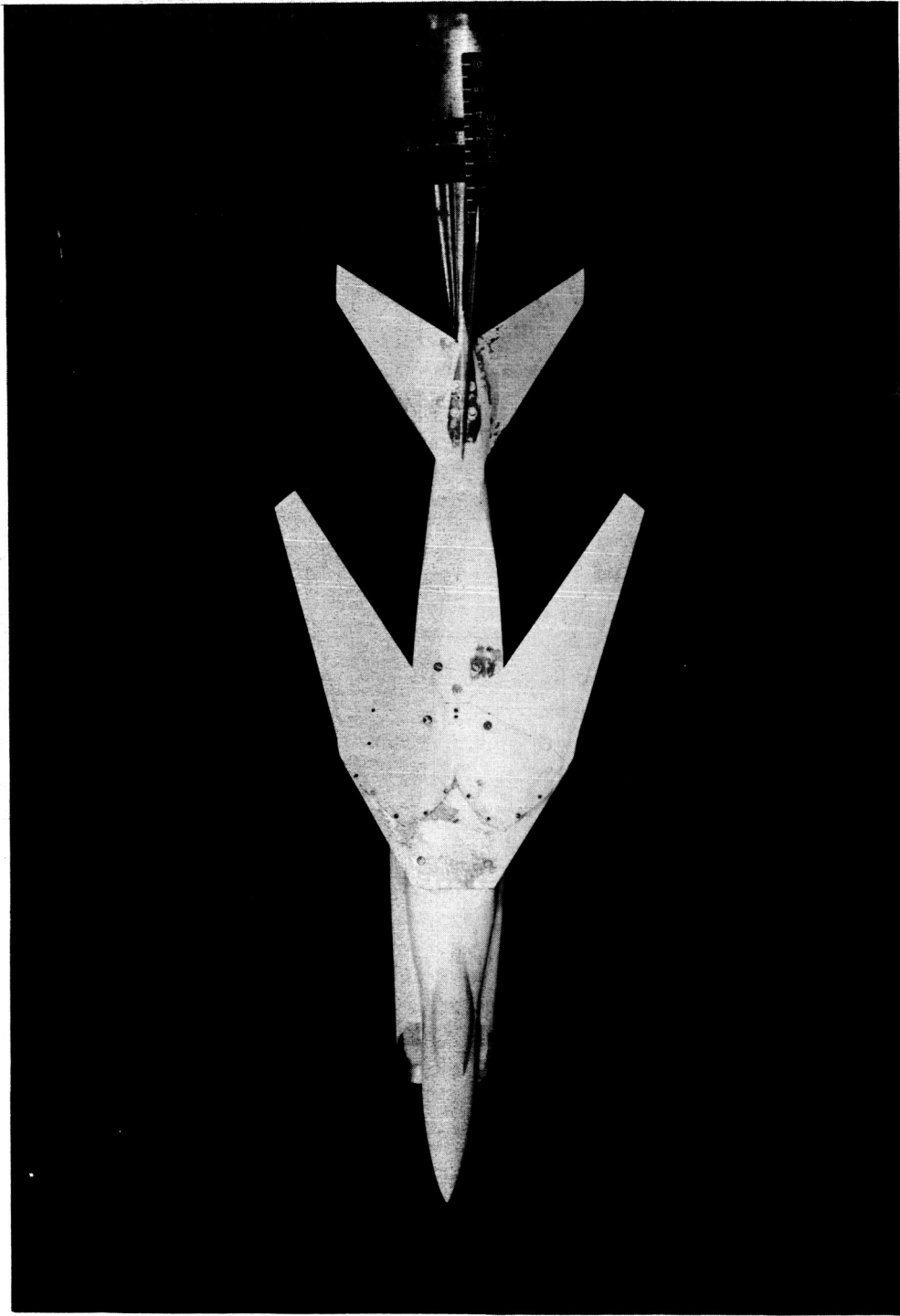
(a) Top view of model with 75° swept wing.   L-60-7014

Figure 2.- Photographs of model configurations.

L-1458

L-1458
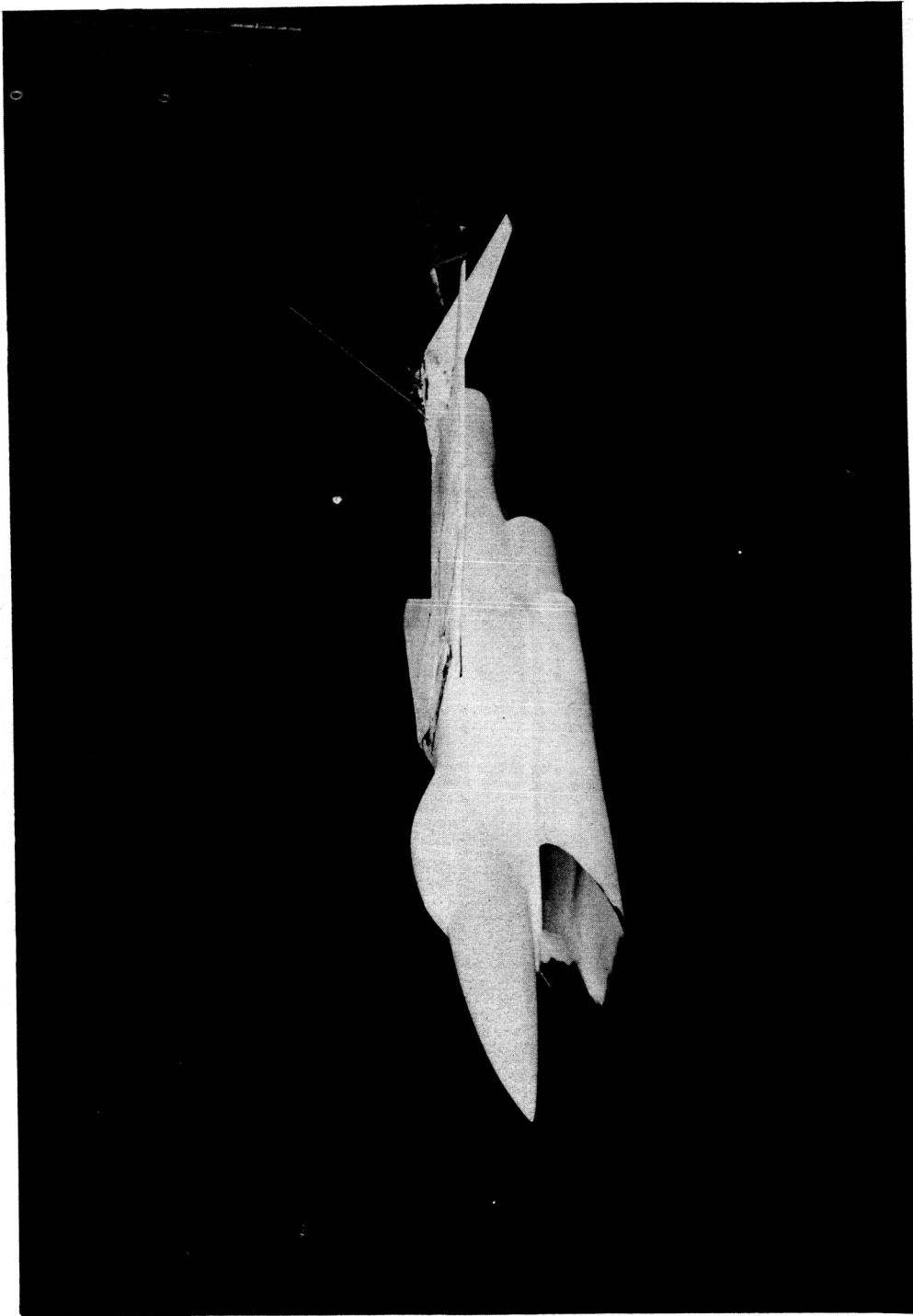
L-60-7015

(b) Photograph of model with 75° swept wing showing inlet.
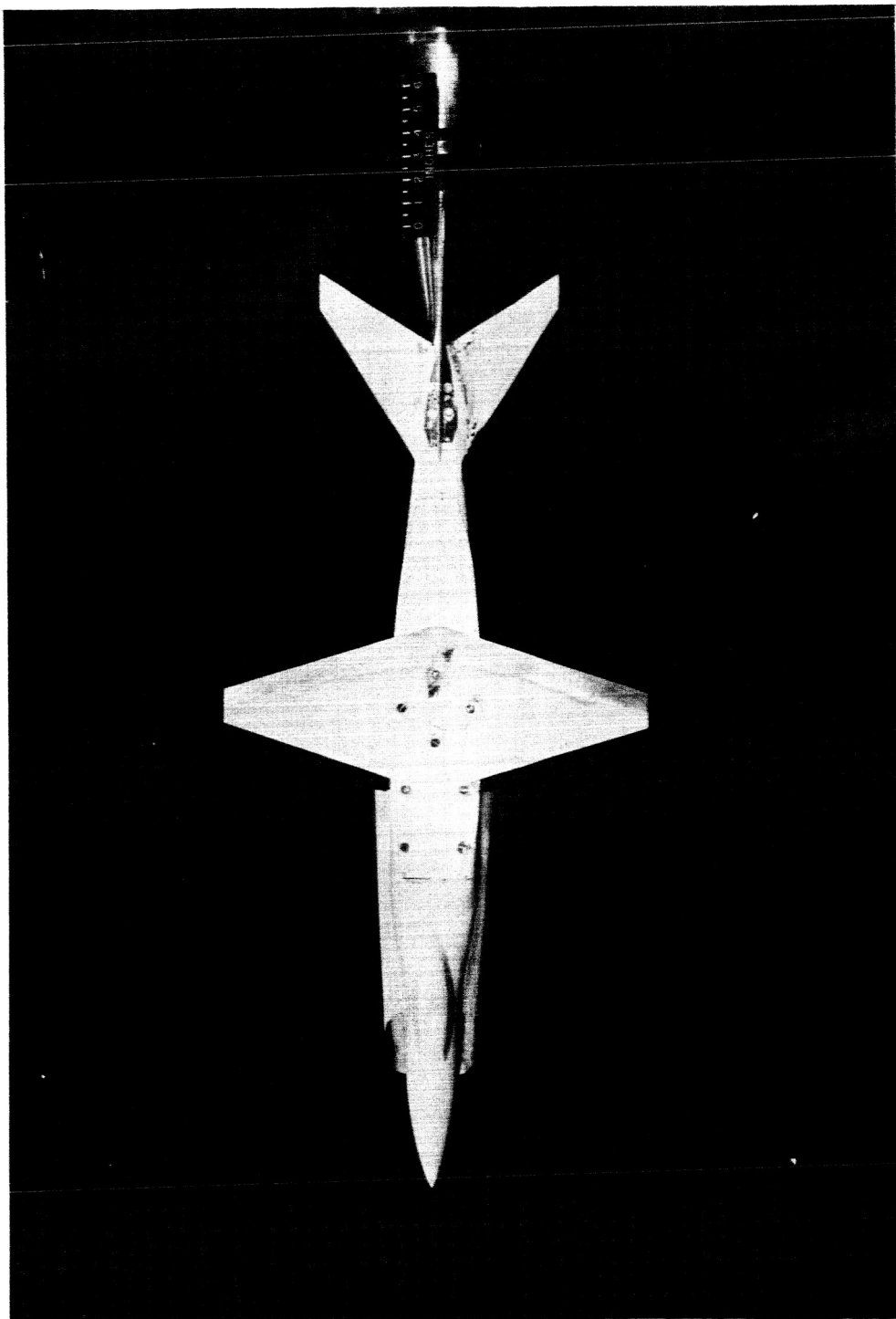
Figure 2.- Continued.

(c) Top view of model with skewed wing at 0°.

Figure 2.- Continued.

L-1458
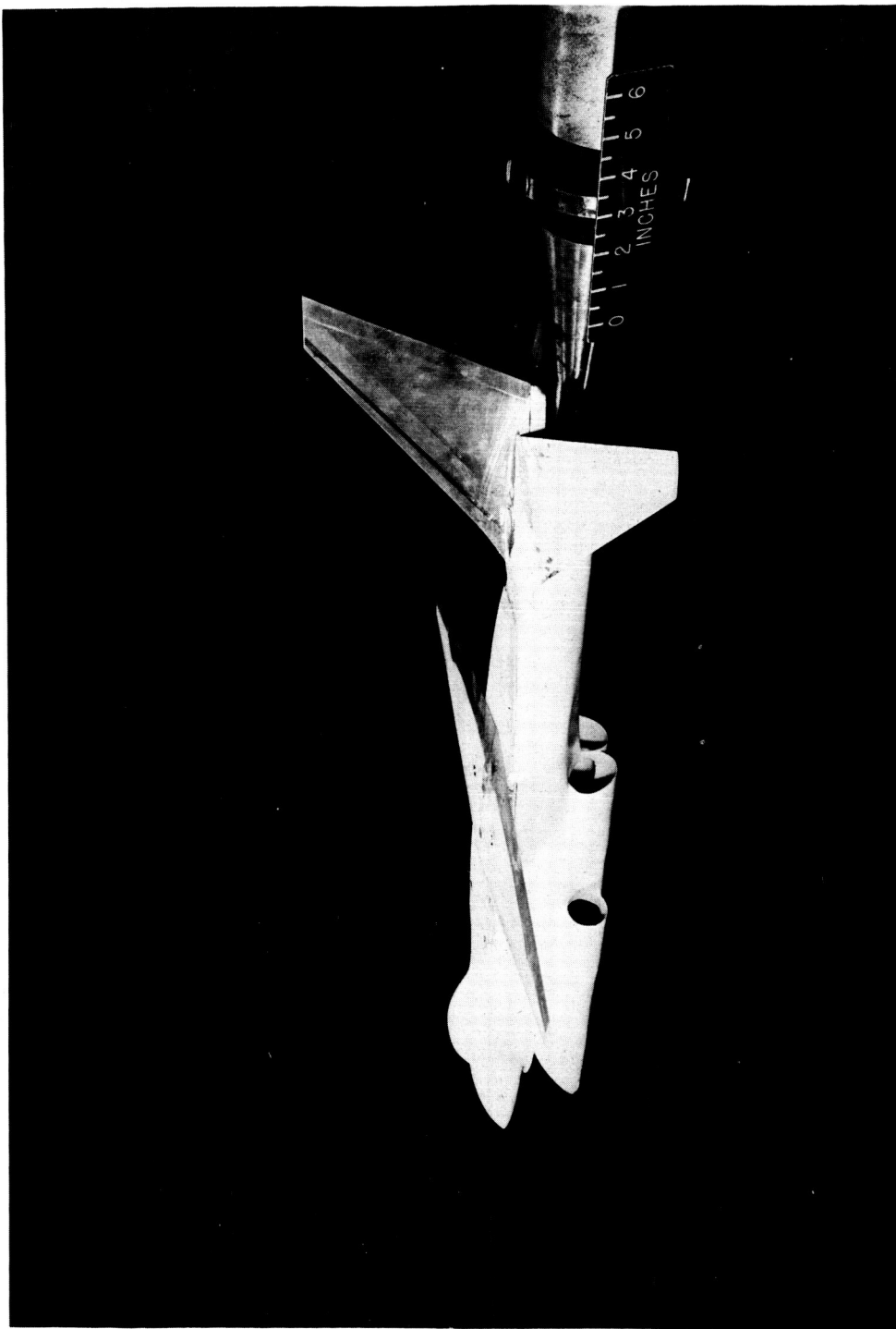
(d) Photograph of model with skewed wing showing nacelle exits. L-60-7016

Figure 2.- Concluded.
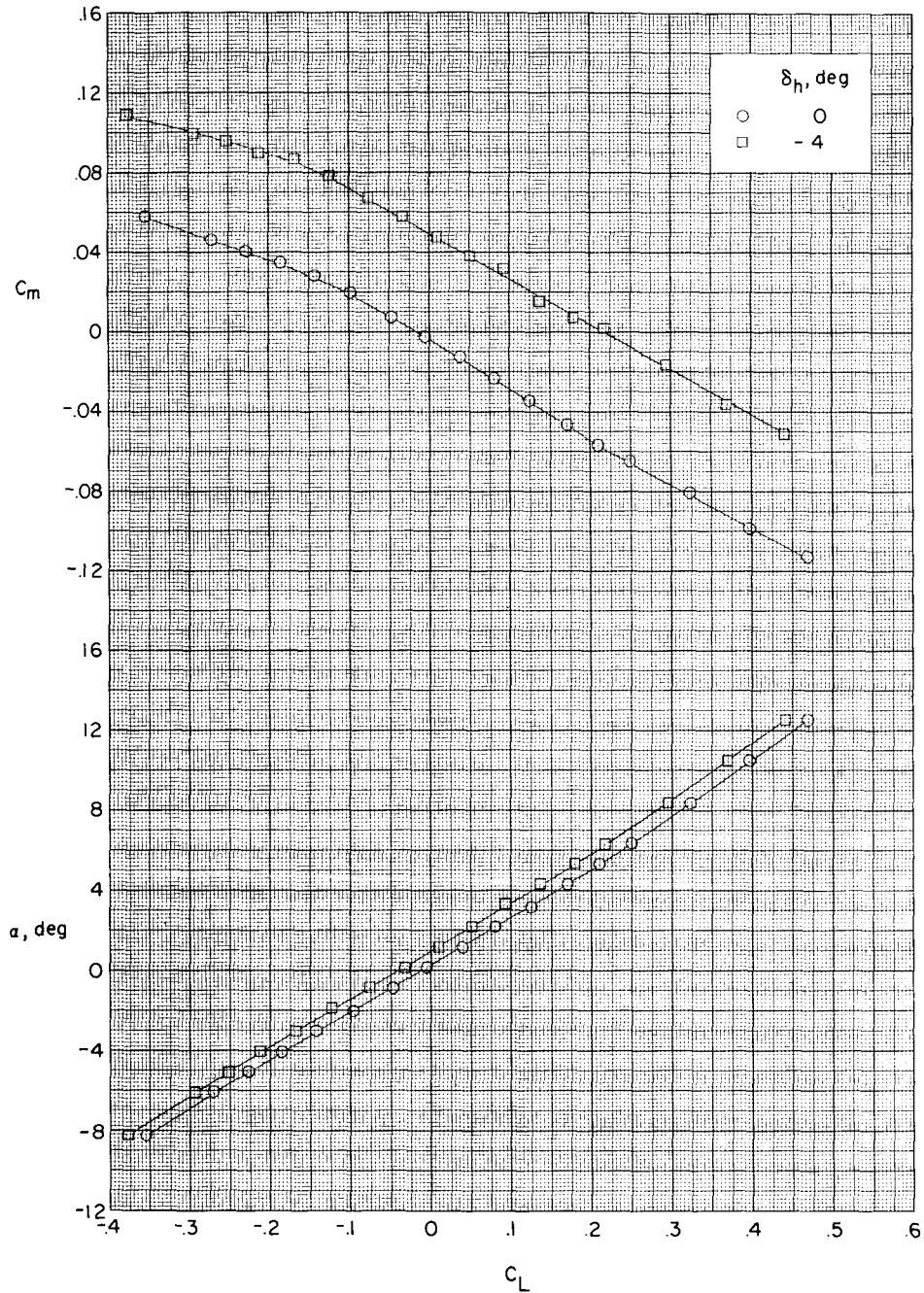
(a) Variation of C_m and α with C_L.

Figure 3.- Effect of horizontal-tail deflection on the aerodynamic characteristics in pitch for configuration with 75° swept wing.

L-1458
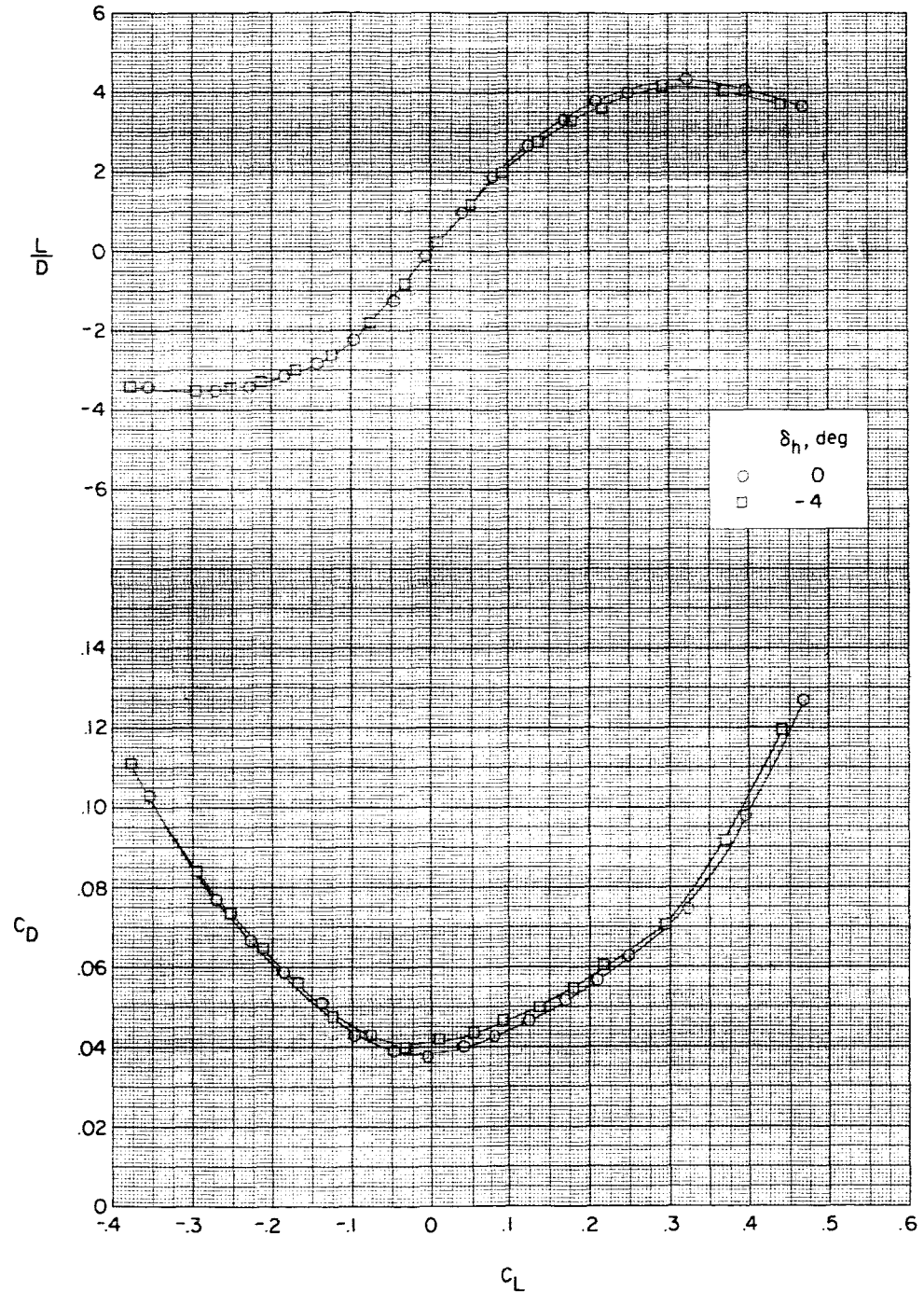
(b) Variation of L/D and C_D with C_L.

Figure 3.- Concluded.
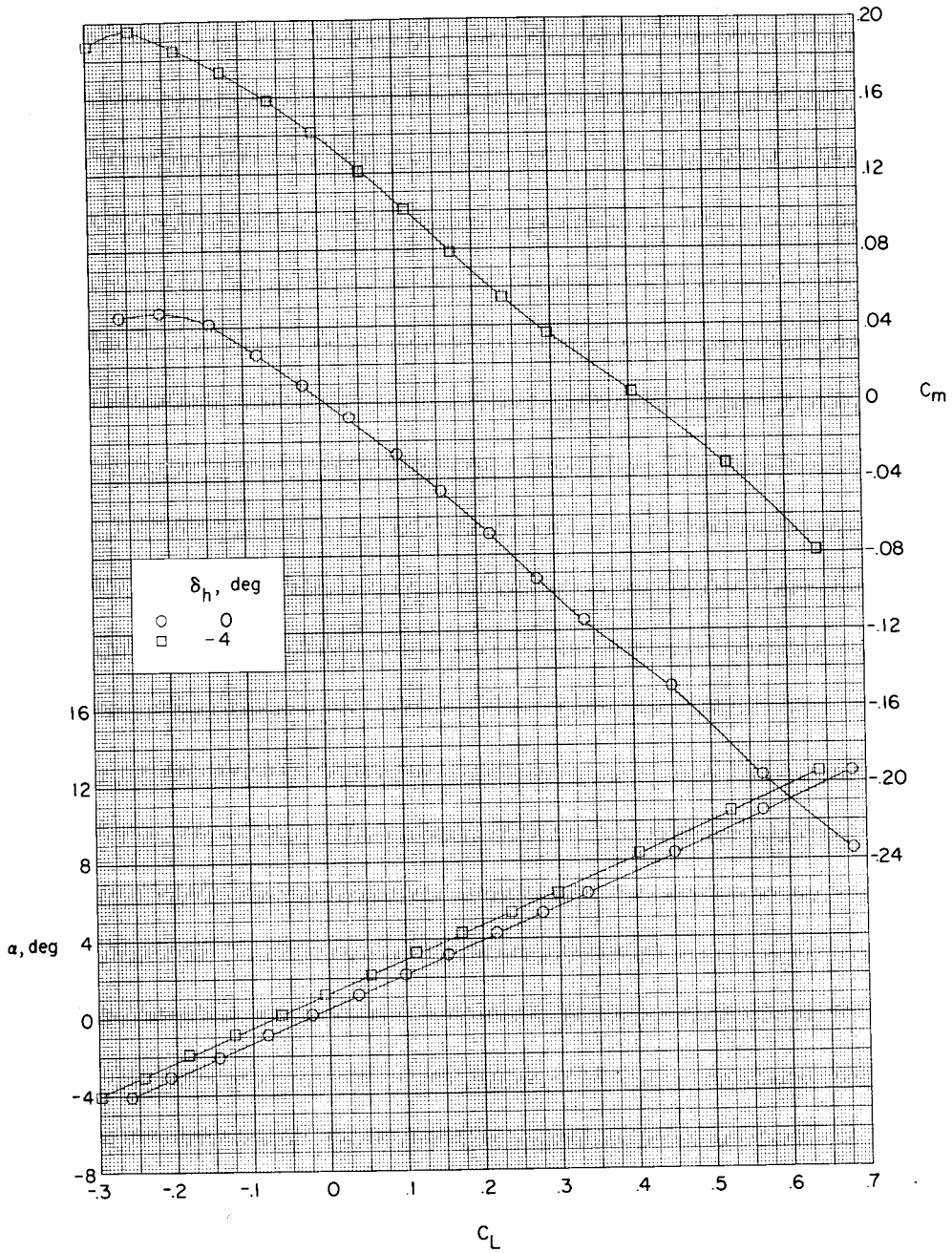
(a) Variation of C_m and α with C_L.

Figure 4.- Effect of horizontal-tail deflection on the aerodynamic characteristics in pitch for the configuration with 0° skewed wing.
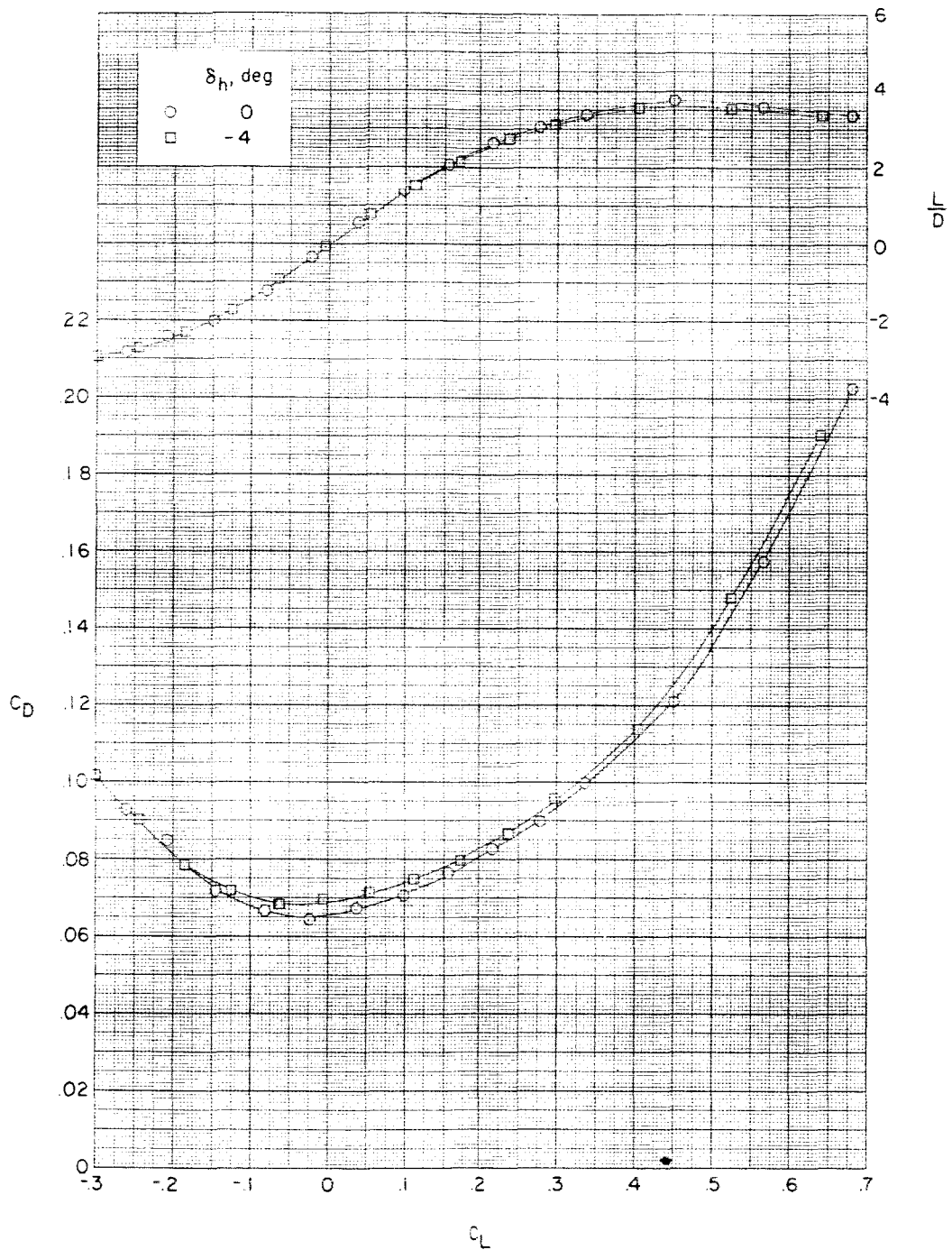
L-1458

(b) Variation of L/D and C_D with C_L.

Figure 4.- Concluded.
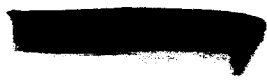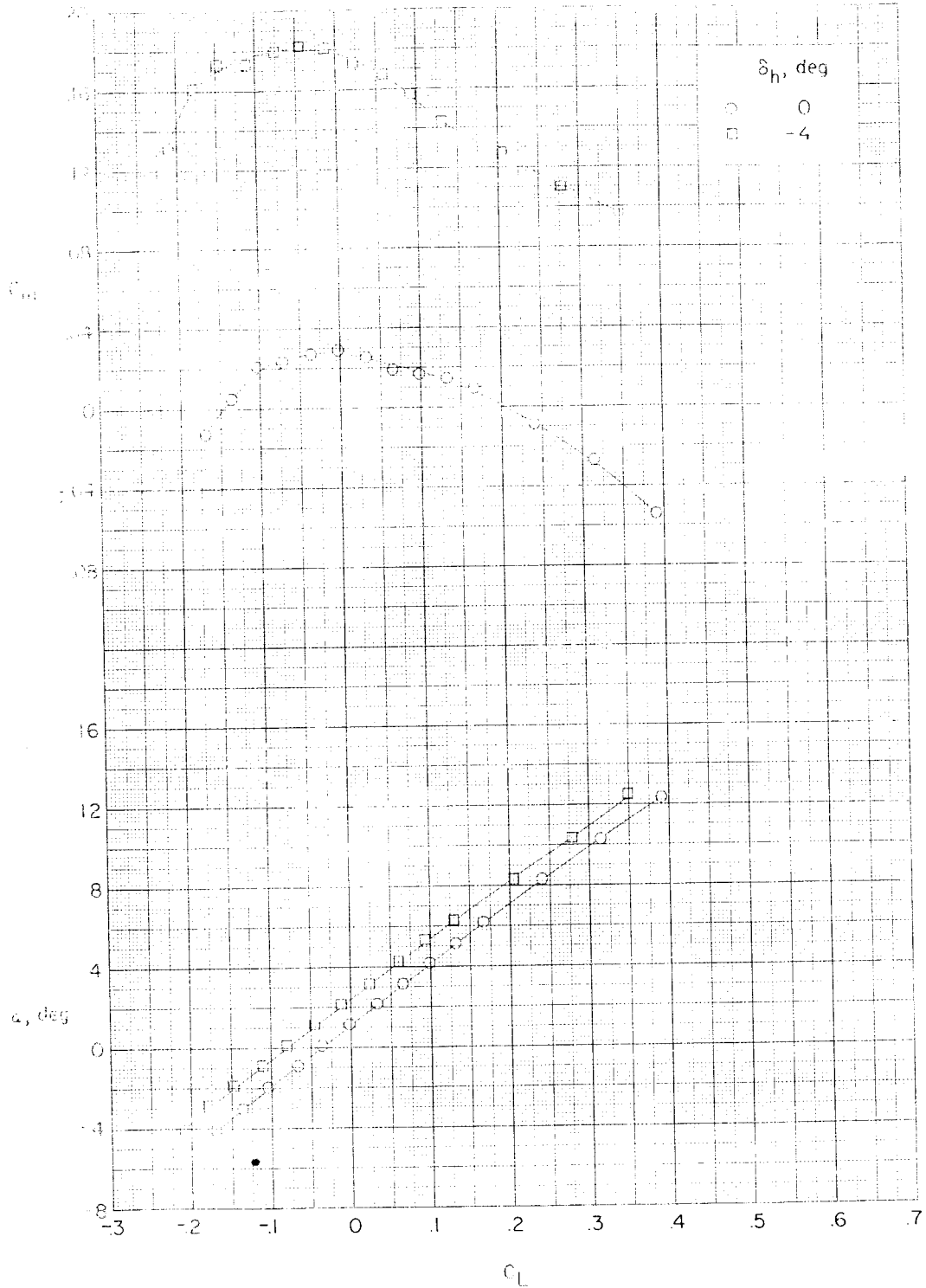
(a) Variation of C_m and α with C_L.

Figure 5.- Effect of horizontal-tail deflection on the aerodynamic characteristics in pitch for the configuration with 20° skewed wing.

L-1458
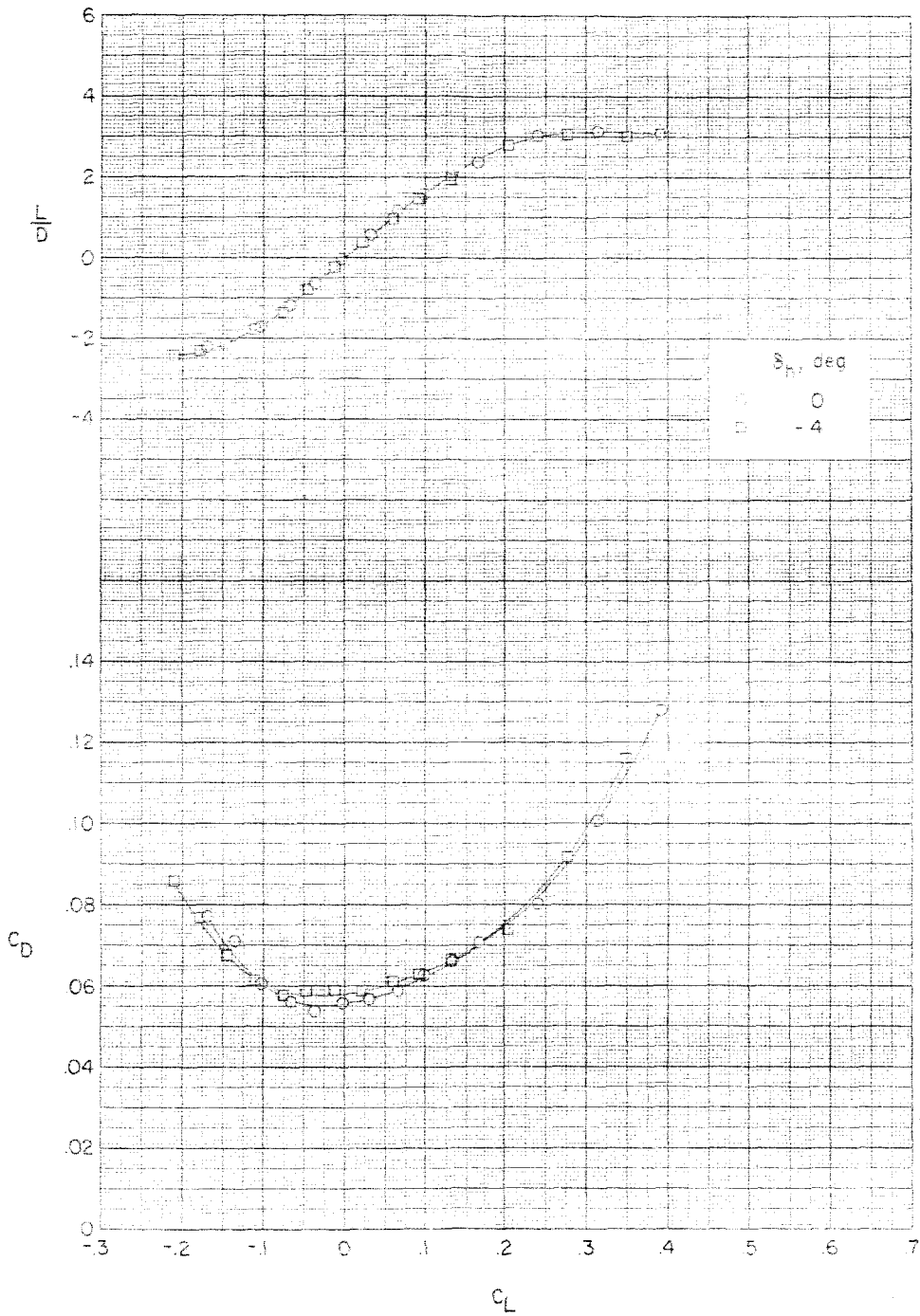
(b) Variation of L/D and C_D with C_L.

Figure 5.- Concluded.
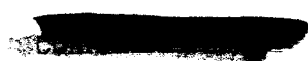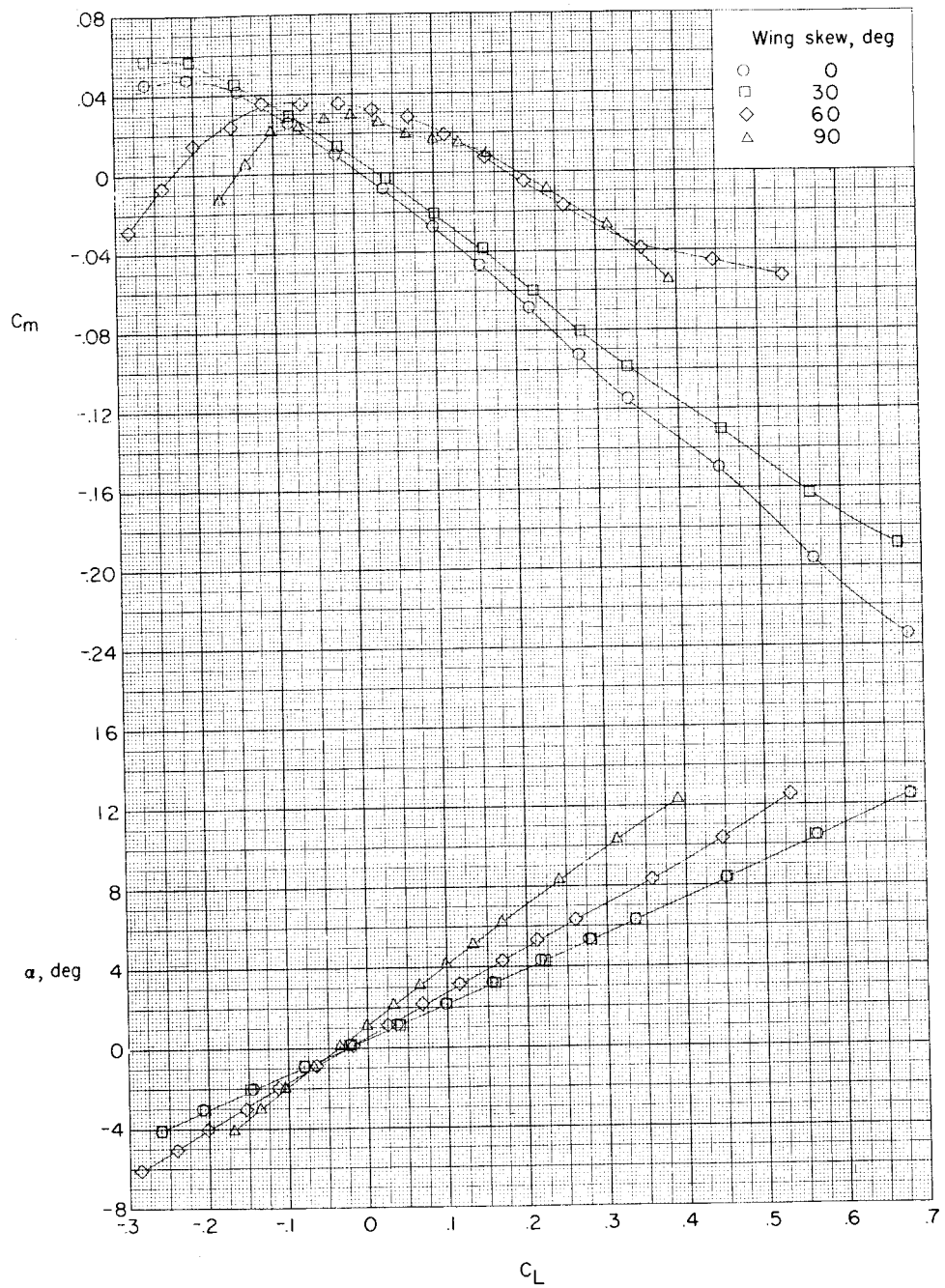
(a) Variation of C_m and α with C_L.

Figure 6.- Effect of wing skew on the aerodynamic characteristics
in pitch for the skewed-wing configuration.

L-1458
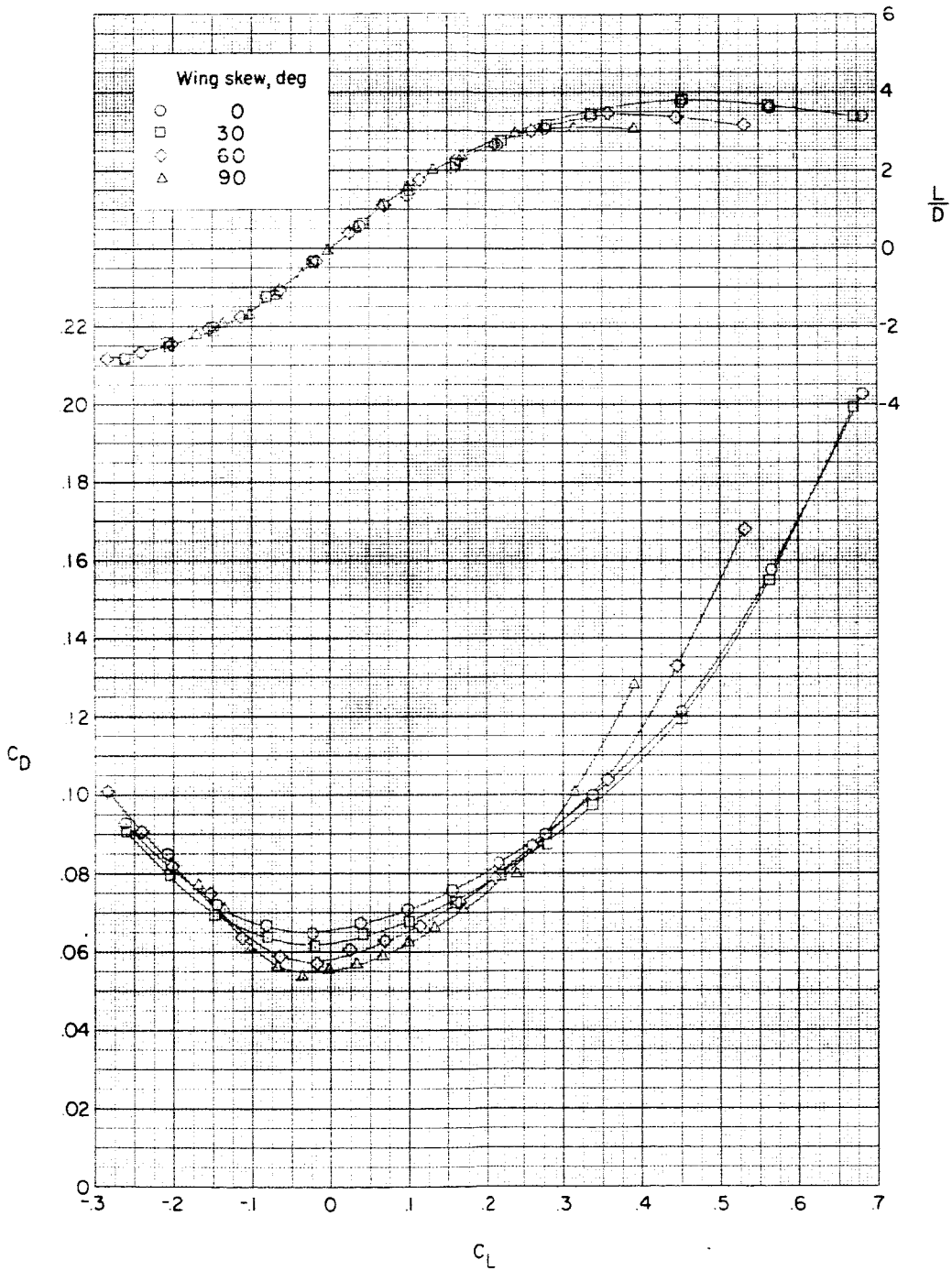
(b) Variation of L/D and C$_D$ with C$_L$.

Figure 6.- Concluded.
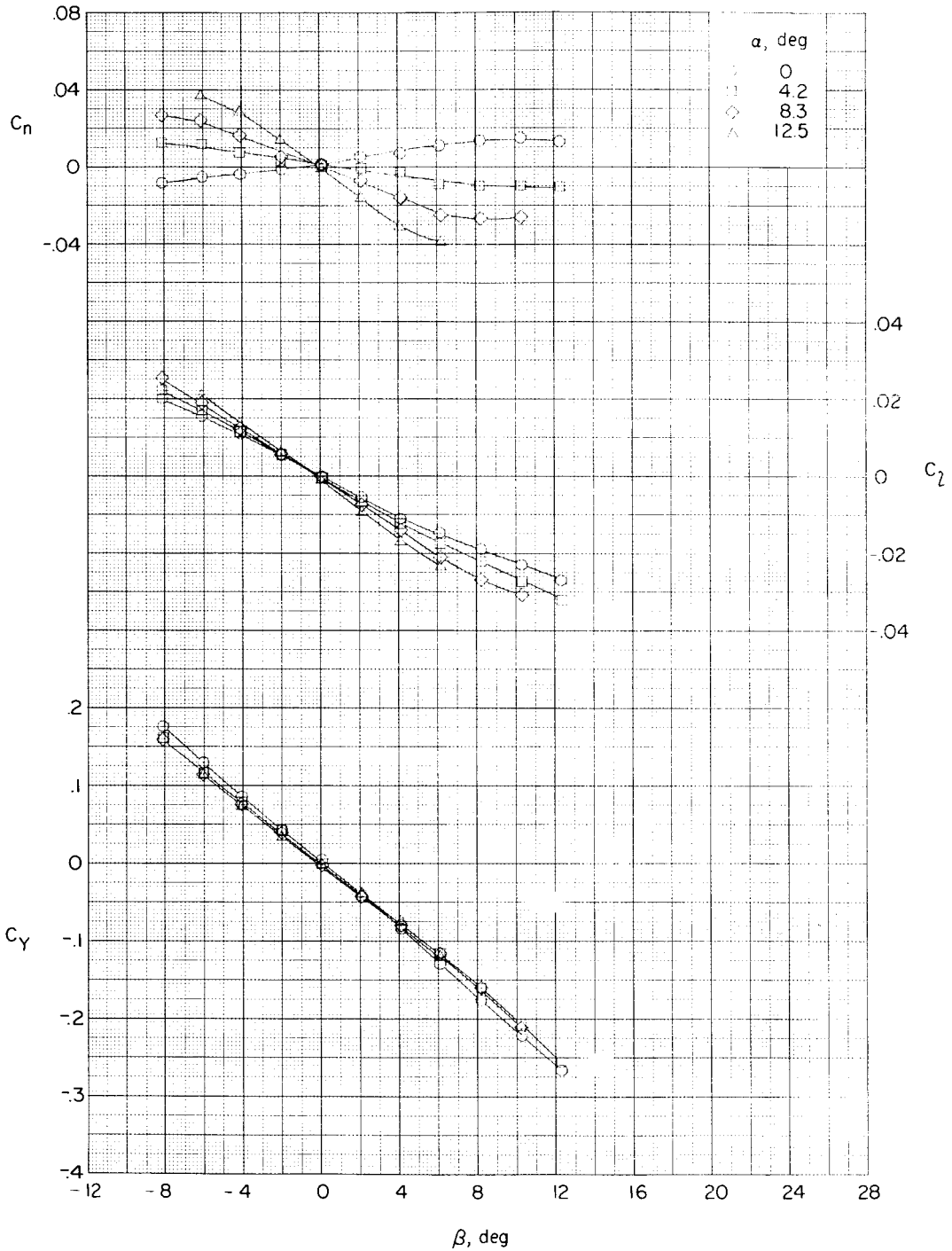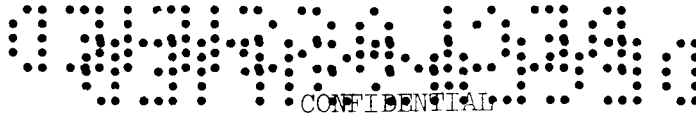
Figure 7.- Variation of the aerodynamic characteristics in sideslip for configuration with 75° swept wing.

(a) $\alpha = 0^o$.
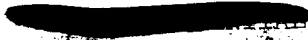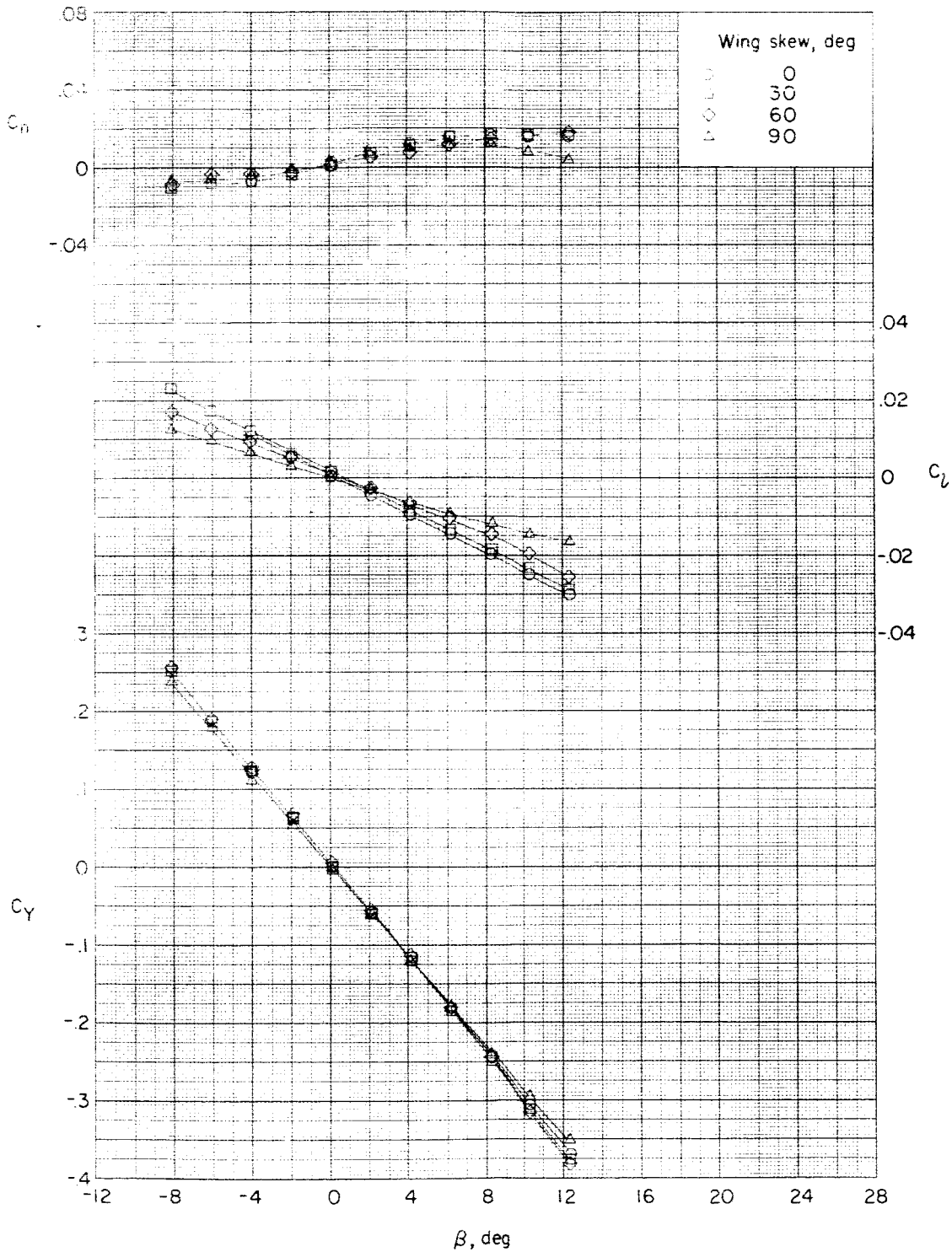
Figure 8.- Effect of wing skew on the aerodynamic characteristics in sideslip for the skewed-wing configuration.
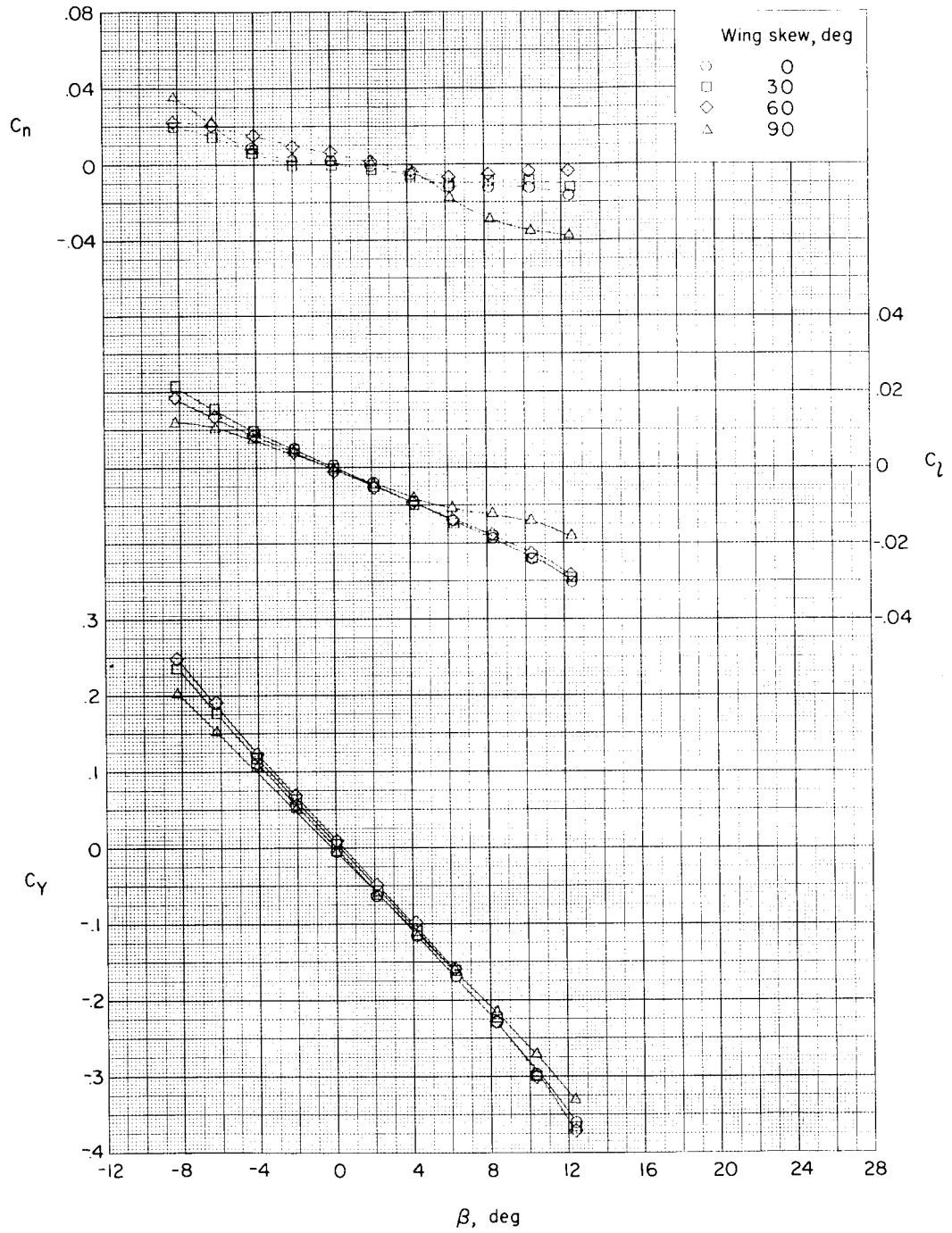
(b) $\alpha = 4.2°$.

Figure 8.- Continued.

L-1458

CONFIDENTIAL

25

L-14740
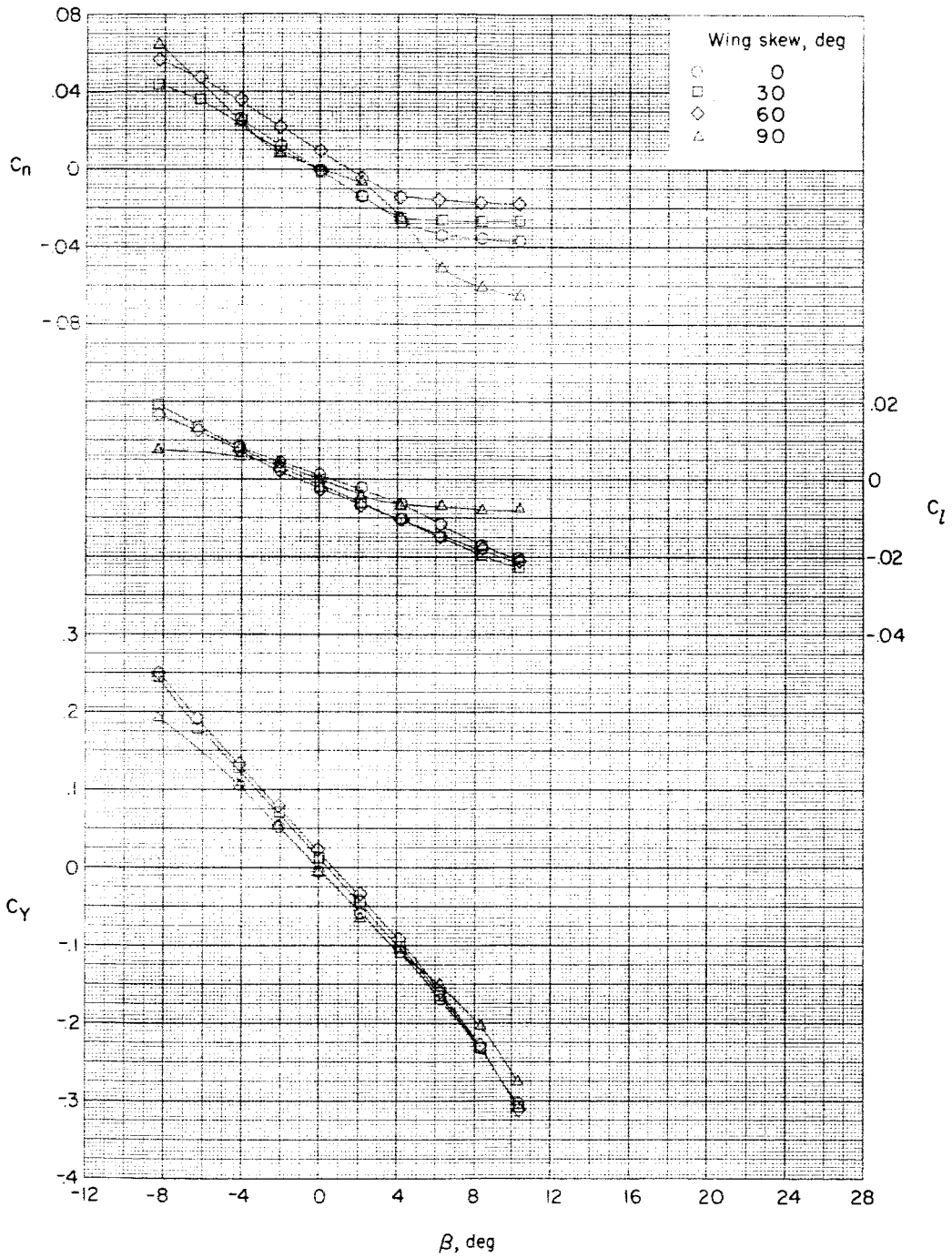
(c) $\alpha = 8.3°$.

Figure 8.- Continued.
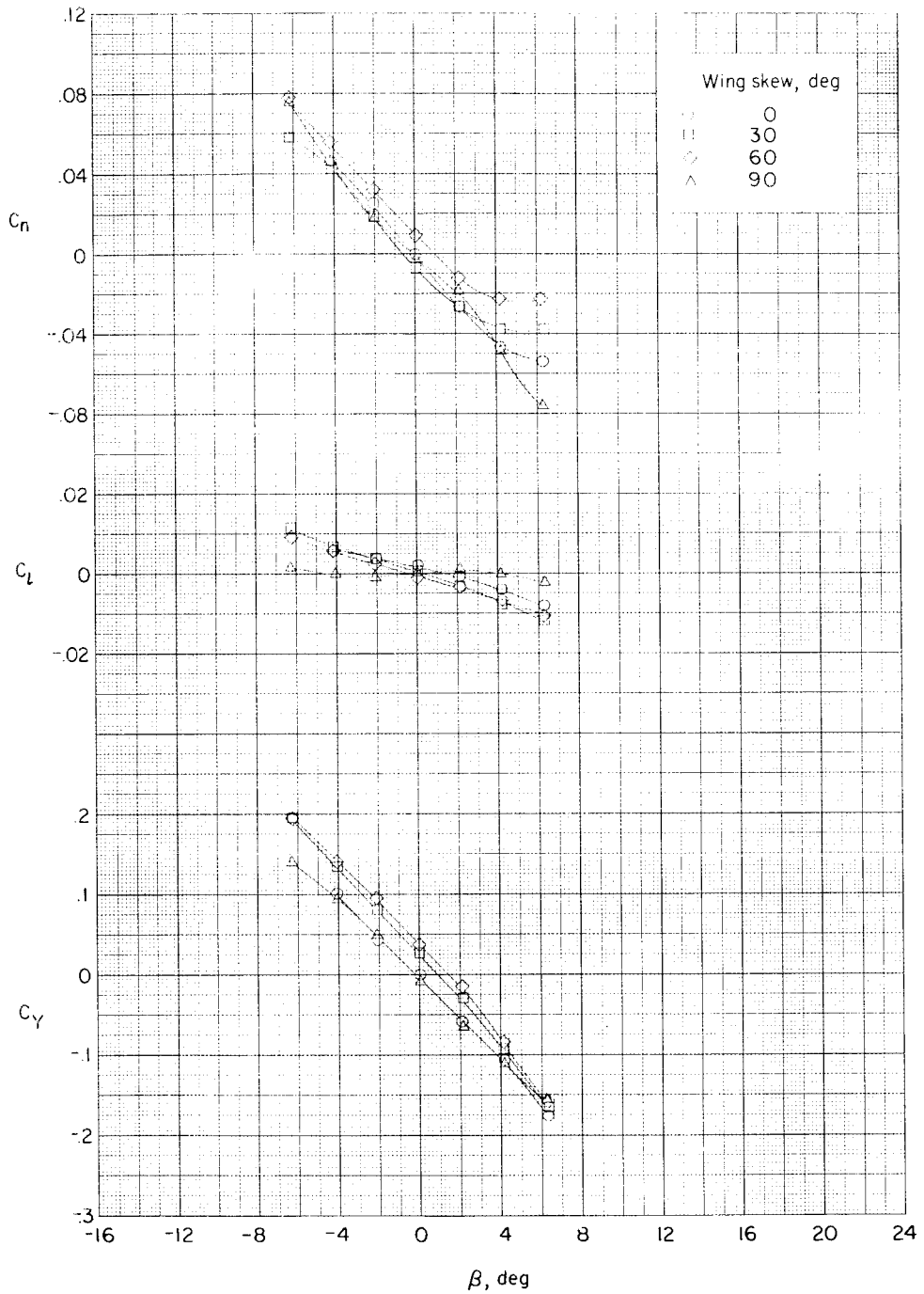
(d) $\alpha = 12.5^\circ$.

Figure 8.- Concluded.
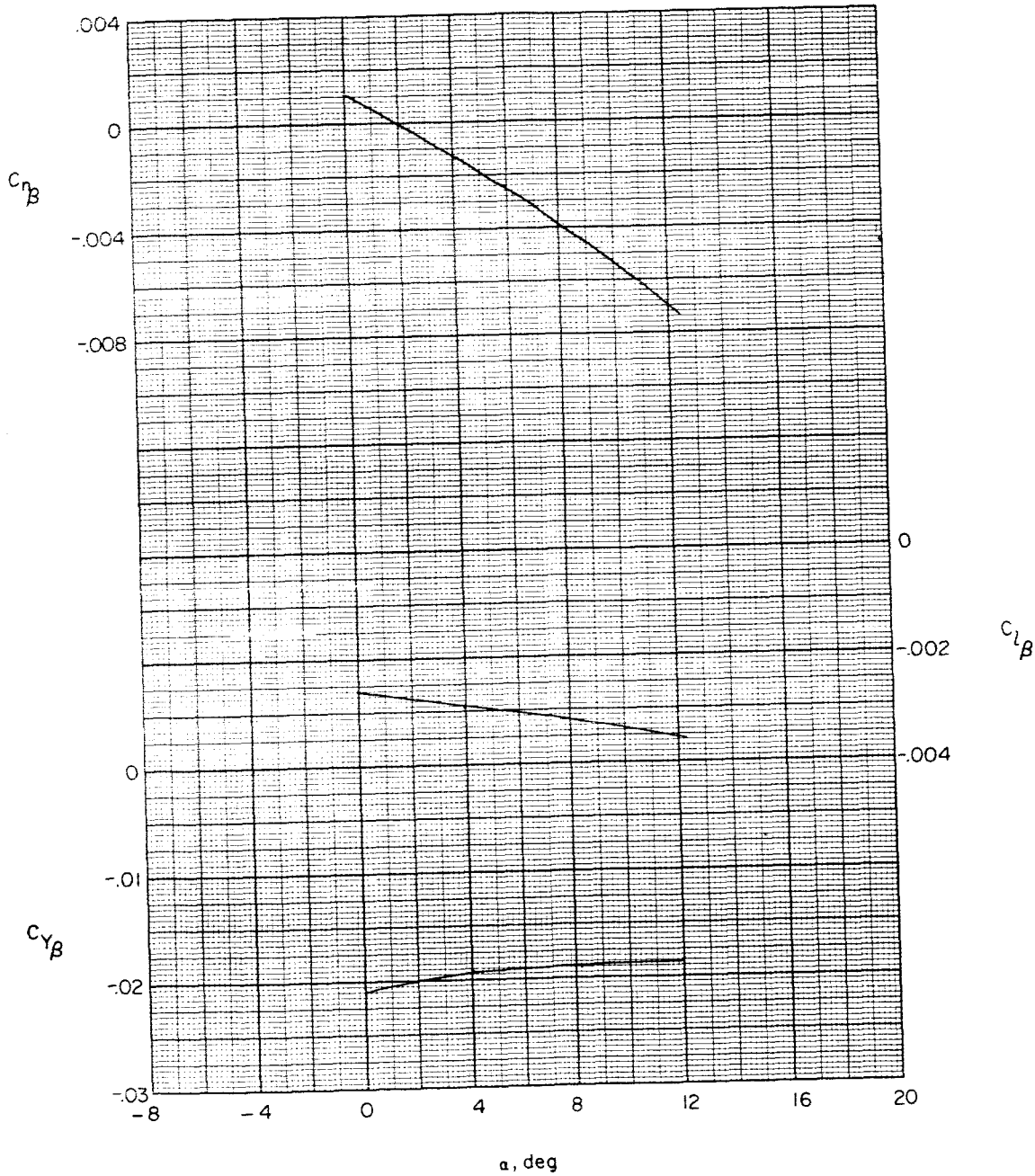
Figure 9.- Variation of the lateral-stability derivatives with angle of
attack for the configuration with 75° swept wing.
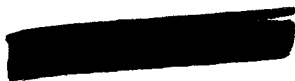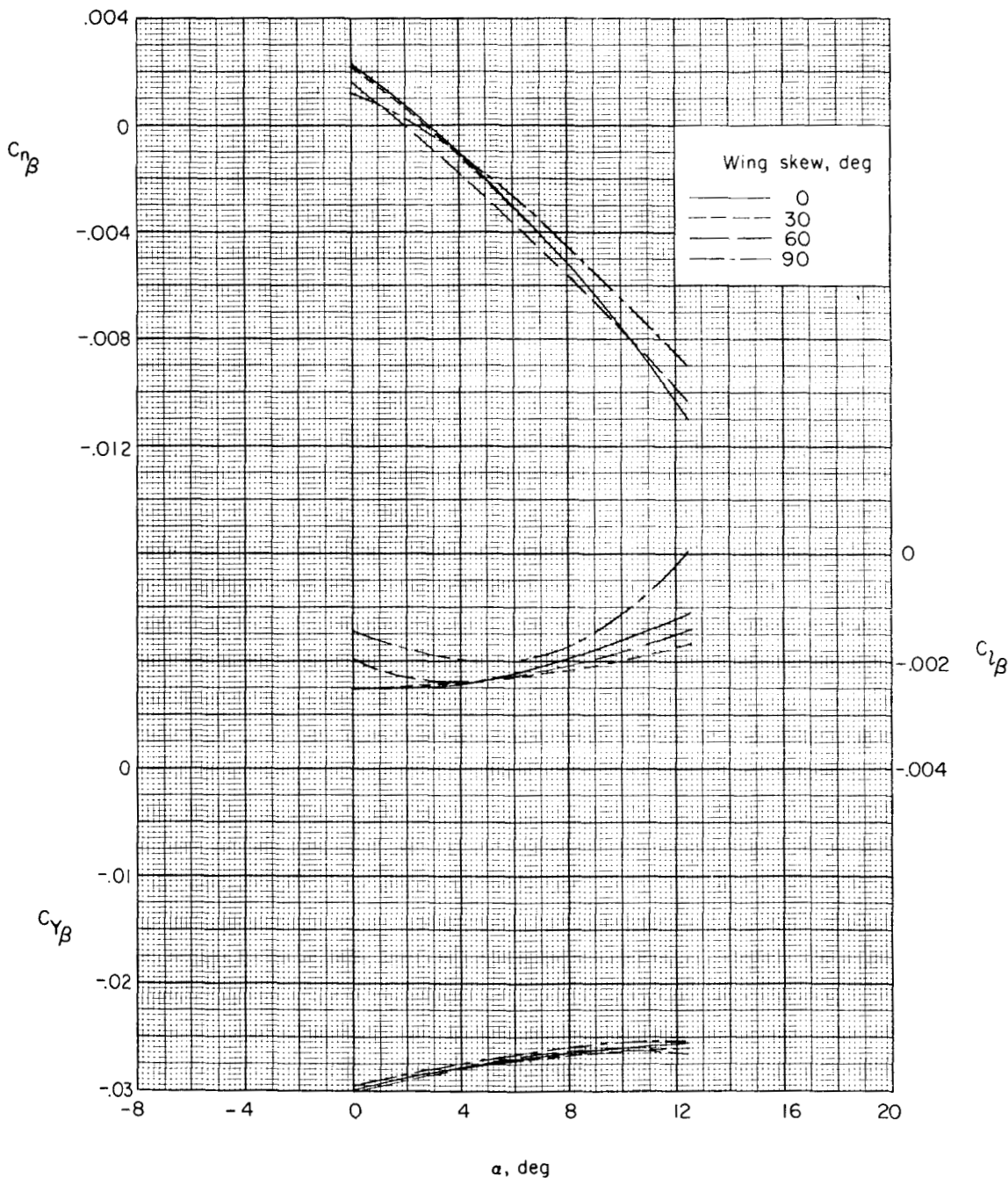
Figure 10.- Variation of the lateral-stability derivatives with angle
of attack for the skewed-wing configuration.